A phenomenological model to describe turbulent friction in permeable-wall flows

A phenomenological model to describe turbulent friction in permeable-wall flows

C. Manes,[1] L. Ridolfi,[2] and G. Katul[3]

Received 13 May 2012; revised 15 June 2012; accepted 15 June 2012; published 27 July 2012.

[1] Describing the canonical properties of turbulent flows over rough-permeable walls such as gravel beds, vegetated- or snow-covered surfaces have, to date, resisted complete theoretical treatment. The major complication in describing such geophysical flows is that the friction factor - Reynolds number relationships significantly deviate from their conventional Nikuradse curves or Moody diagrams derived over impermeable rough boundaries. A novel phenomenological model that describes such anomalous behavior is proposed. It expands the approach in Gioia and Chakraborty (2006) developed for rough-impermeable pipes to include finite velocity effects within the porous wall and canonical length scales governing the momentum exchanges between interstitial and superficial flows. **Citation:** Manes, C., L. Ridolfi, and G. Katul (2012), A phenomenological model to describe turbulent friction in permeable-wall flows, *Geophys. Res. Lett.*, *39*, L14403, doi:10.1029/2012GL052369.

1. Introduction

[2] Numerous geophysical applications requiring the description of bulk flow over rough surfaces employ the so-called Darcy-Weisbach equation, a phenomenological equation that relates the total energy loss due to friction along a given pipe length to the time- and area-averaged velocity V via a so-called friction factor f. The Darcy-Weisbach equation, named after two hydraulic engineers of the middle 19th century, is now accepted as the best empirical relationship to be used for pipe-flow resistance computations when employed with the Nikuradse experiments or the Moody diagram describing f. These seminal experiments of Nikuradse [*Nikuradse*, 1933], now routinely used in all types of wall-bounded flows, were among the first to describe f as a function of (i) the bulk Reynolds number ($Re = VR/\nu$, R is the radius of the pipe and ν is the kinematic viscosity) and (ii) the relative roughness ratio R/r (r is a characteristic roughness size). In fact, it is precisely those early experiments and the compact representation offered by the Moody diagram representation of the f-Re relation in the mid 1940s that enabled wide-usage of the Darcy-Weisbach equation first in hydraulic engineering and later on in the geosciences (especially in hydrology). However, Nikuradse's experiments were carried out in rough-impermeable pipes whereas a large number of geophysical applications require V over permeable-rough walls. These applications include the modelling of flow resistance in rivers characterized by gravel or vegetated beds or atmospheric flows over forests or snow. Specifically, this work is most pertinent to the hyporheic zone, a zone beneath or alongside a stream bed where mixing between shallow groundwater and surface water occurs. The flow dynamics and concomitant mass and energy transfer in this zone remains central to determining surface water/groundwater interactions and stream ecology.

[3] A permeable wall differs from an impermeable one because the finite permeability allows momentum penetration within the wall at scales larger than the characteristic size of its constitutive components (e.g., grains diameter). In the case of a granular impermeable wall, momentum penetration can be limited by the grain diameter, whereas in a permeable granular wall, momentum penetration is deeper because the wall thickness is significantly larger than the grain diameter. Some experiments have already demonstrated that f in rough-permeable walls differ from their impermeable counterparts, especially when Re is large [*Ruff and Gelhar*, 1972; *Zagni and Smith*, 1976; *Zippe and Graf*, 1983; *Manes et al.*, 2011]. The number of experiments dedicated to this subject remains limited; however, these experiments share a number of common features. For a fixed immobile permeable wall, these experiments show that f follows a typical "s-shaped" curve characterized by a standard transitional regime at low Re, a plateau at intermediate Re, and a further rising regime for higher Re (Figure 1). The results of *Manes et al.* [2011] also show that the plateau occurs at friction factors f corresponding to the hydraulically rough regime of an equivalent impermeable wall having the same relative roughness. The rising regime is therefore a peculiar characteristic of permeable walls since for impermeable rough walls the plateau persists with increasing Re. In fact, $\partial f/\partial Re = 0$ generally delineates the so-called hydraulically rough regime in impermeable walls. In previous studies, the rising regime was explained as an effect of momentum penetration within the wall and/or persistent viscous effects on the drag around buried or sheltered roughness elements [*Manes et al.*, 2011; *Zagni and Smith*, 1976]. Recently, *Manes et al.* [2011] argued that momentum penetration within the wall increases with increasing Re and this is equivalent to an increase in the effective wall roughness, which ultimately leads to higher f. Furthermore they have argued that, within the momentum penetration depth, viscous forces contribute significantly to the total drag acting on sheltered or buried particles because of the reduced local Reynolds number. This then contributes to the

[1]Energy and Climate Change Research Unit, School of Engineering and the Environment, University of Southampton, Southampton, UK.
[2]Dipartimento di Idraulica, Trasporti ed Infrastrutture Civili, Politecnico di Torino, Turin, Italy.
[3]Nicholas School of the Environment, Duke University, Durham, North Carolina, USA.

Corresponding author: C. Manes, Energy and Climate Change Research Unit, School of Engineering and the Environment, University of Southampton, Highfield, Southampton SO19 1BJ, UK. (c.manes@soton.ac.uk)

0094-8276/12/2012GL052369

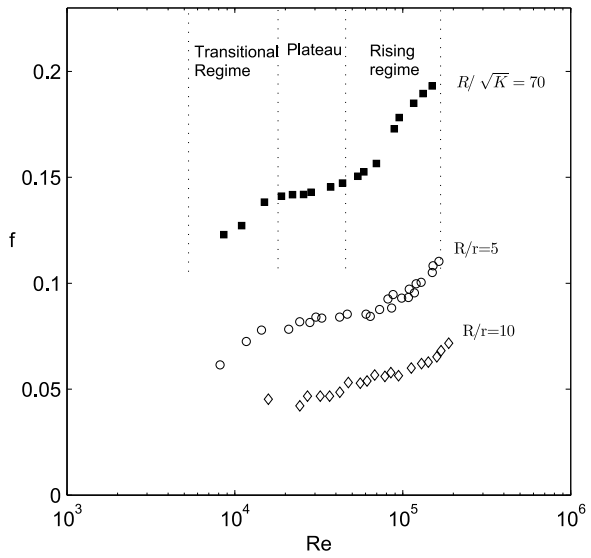

Figure 1. Measured friction factor f curves for pipe flow with permeable walls as a function of the bulk Reynolds number Re: solid and hollow symbols refer to polyurethane foam and granular walls, respectively [*Ruff and Gelhar*, 1972]; K is the wall permeability; R/r is the ratio between pipe radius and roughness size. The foam experiment is classified with the ratio $R/\sqrt{K}$ instead of the most commonly used R/r, because polyurethane foams do not have a well defined size of roughness elements r like granular walls do. Note the occurrence of the (anomalous) rising regime after the occurrence of a plateau.

dependency of f on Re even at values of Re for which the hydraulically rough regime is expected.

[4] Despite these advances, a phenomenological description of the rising regime remains qualitative and has resisted complete theoretical treatment. This issue frames the compass of this work and is addressed via a proposed phenomenological model. The model makes use of well established laws for drag parametrization in porous media at high Reynolds numbers and builds upon the work of *Gioia and Chakraborty* [2006, hereinafter GC06], developed to describe the Nikuradse experiments.

2. Theoretical Background

[5] For a steady and uniform flow over impermeable rough walls, GC06 argue that eddies responsible for momentum exchange with the wall surface are those that straddle the coves between successive roughness elements. The size of these eddies is estimated as $s = r + m\eta$, where r is, as before, the characteristic size of the roughness elements and $m\eta$ is the viscous layer thickness, with η being the Kolmogorov dissipation length scale and $m(\simeq 5)$ is a conventional constant derived from boundary layer theory over smooth flat plates [*Pope*, 2000]. For $Re \to \infty$, s tends to r as η becomes very small (recall that η/R scales as $Re^{-3/4}$). The wall shear stress can be estimated as $\tau_0 = \rho\kappa_\tau V u_s$, where ρ is the fluid density and u_s is a characteristic turnover velocity associated with an eddy of size s (κ_τ is a constant of order 1). GC06 estimated $u_s^2 = \int_0^s E(\sigma)d\sigma$ where, $E(\sigma) = A\varepsilon^{2/3}\sigma^{5/3}c_d(\eta/\sigma)c_e(\sigma/R)$, A is a dimensionless constant (that can be related to the Kolmogorov constant), ε is the turbulent kinetic energy dissipation rate, $\eta = \nu^{2/3}\varepsilon^{-1/4}$ is, as before, the Kolmogorov dissipation length scale, $A\varepsilon^{2/3}\sigma^{5/3}$ is the conventional Kolmogorov spectrum, which is valid for eddy sizes s in the inertial range where $\eta \ll s \ll R$, $c_d = \exp(-\beta\eta/\sigma)$ and $c_e = [1 + \gamma(\sigma/R)^2]^{-17/6}$ are correction functions for the dissipation and production range respectively when s becomes commensurate with η or R, with β and γ being two dimensionless constants [*Pope*, 2000]. Starting from its definition, f can hence be computed as $f = 8(u_*^2/V^2)$, where $u_* = \sqrt{\tau_0/\rho}$ and hence $f = 8(\kappa_\tau u_s/V)$. Calculating f requires knowledge of u_s and hence integrating the spectrum $E(\sigma)$ within a domain of length scales smaller than s. GC06 showed that Nikuradse's curves can be explained in terms of the scale of eddies dominating momentum transport and their position within the different regions of the velocity spectrum (i.e., production, inertial and dissipation region) with increasing Re.

[6] For the smooth and transitional regime, the GC06 model is likely to be valid for both permeable and impermeable boundaries because the roughness elements are buried within a continuous viscous sub-layer and hence turbulence penetration is damped and momentum transfer is dominated by eddies scaling with s. With increasing Re, large-scale structures (i.e., those larger than r) populating the near-wall region become energetic enough to penetrate the permeable bed. Such structures are responsible for exchanging momentum between the fast-moving fluid above the wall and the slow-moving fluid within the permeable wall, across a penetration depth $\delta_e > s$ (see Figure 2). It follows that the shear stress acting over the fluid-wall interface must be the sum of two contributions, i.e., $\tau_0 = \tau_s + \tau_p$, where $\tau_s = \rho\kappa_\tau V u_s$ is associated with momentum

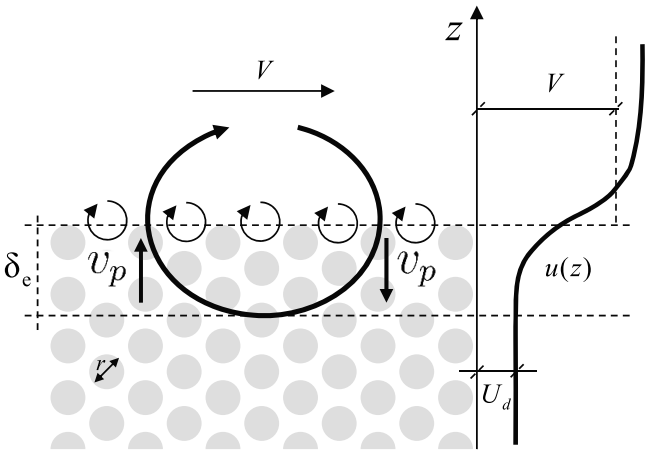

Figure 2. (left) Conceptual scheme of the momentum transfer over a permeable wall. The small eddies are selected by the roughness element length scale and contribute to τ_s as modelled by GC06. Differently, the large eddy here represents the turbulent coherent structures able to penetrate across a depth δ_e (i.e., the turbulence penetration depth) into the wall and contribute to τ_p; v_p is the vertical velocity component imposed by the large eddies within the wall; U_d is the interstitial velocity within the shear-free flow region; V is the depth-averaged velocity; r is the characteristic size of the roughness elements. (right) The qualitative behavior of the time-averaged velocity profile $u(z)$ is also shown.

transport induced by the eddies straddling the roughness coves (and calculated using the GC06 model) whereas τ_p takes into account the effects of permeability and the turbulent momentum transport induced by large scale eddies. Define v_p as the vertical velocity component of the fluid moving across the penetration depth δ_e sustained by the large turbulence structures; U_d is the uniform velocity of the interstitial fluid resulting from a force balance between the mean pressure gradient, the weight of the fluid, and the opposing drag force acting on the fluid by the solid elements (Figure 2); as for the impermeable wall case, V remains the bulk velocity of the flow outside the wall. Large scale eddies contribute to the wall shear stress via sweeps and ejections that inject fast moving fluid within the bed and extract slow moving fluid from the bed, respectively. Then the total momentum flux due to sweeps and ejections can be thought of as a mass flux crossing the fluid wall interface, multiplied by a velocity contrast, i.e., $\tau_p \propto \rho\phi v_p(V - U_d)$ where ϕ is the bulk porosity of the wall. The total shear stress at the wall boundary becomes $\tau_0 = \rho\kappa_\tau V u_s + \rho\kappa_p\phi v_p(V - U_d)$, where κ_p is a proportionality constant. The friction factor f can now be determined as:

$$f = 8\left(\kappa_\tau \frac{u_s}{V} + \kappa_p \frac{\phi v_p (V - U_d)}{V^2}\right). \quad (1)$$

To calculate f, it becomes necessary to define v_p and U_d (both non-existing in the GC06 model). The U_d varies with f because it depends on the hydraulic head gradient responsible for moving the fluid within the permeable wall. Assuming that the fluid is forced by a hydraulic gradient S, U_d can be estimated by solving the Forcheimer resistance law $S = aU_d + bU_d^2$ [*Whitaker*, 1996], where $a = \nu/(gK)$, $b = c/(g\sqrt{K})$, K is the permeability of the wall, g is the gravitational acceleration, and c is the so called "Forcheimer term" estimated empirically. A force balance on the fluid volume above the wall results in $u_* = \sqrt{gSR}$; hence, the driving gradient S can be computed as $S = fV^2/(8gR)$. This implies that

$$U_d = \frac{-a + \sqrt{a^2 + 4b\frac{fV^2}{gR8}}}{2b}. \quad (2)$$

The estimation of v_p involves a formulation for the penetration depth δ_e and for the driving force moving the fluid inside and outside the wall across δ_e. Across δ_e, sweeps and ejections impose a kinetic hydraulic head difference $S_p = u_R^2/(2g\delta_e)$, where u_R is the characteristic velocity of such structures. Therefore, in a first-order analysis, the simplest estimate of v_p may be again a Forcheimer resistance law with $S_p = av_p + bv_p^2$. In analogy with GC06, the u_R^2 is derived from the integration of $E(\sigma)$, i.e., $u_R^2 = \int_0^R E(\sigma)d\sigma$, where R (i.e., the pipe radius) is chosen as the representative length scale of large-scale eddies. The penetration depth can be estimated following the work of *Ghisalberti* [2009, hereinafter G09] on obstructed shear flows. Starting from the definition of δ_e being the distance from the wall surface to the level where the fluid shear stress vanishes, G09 showed that δ_e is proportional to the so called drag length scale (or adjustment length scale) of the wall, i.e., $\delta_e \sim \phi(C_d A_f)^{-1}$, where C_d is the drag coefficient of the medium and A_f is the frontal area per unit volume of the solid fraction. More general, the drag length scale can be thought of as the ratio between the square of a chosen scale-velocity V_s and the drag force (per unit mass) acting within the turbulence penetration depth δ_e. In porous media, the drag force can be computed as $DF = (g\phi)(aV_s + b(V_s)^2)$. That is, when the flow is quasi-Darcian, the DF scales linearly with V_s, but as V_s increases, the DF is dominated by the quadratic term, as expected. For simplicity, we chose V as the scale velocity V_s. Other options may involve combinations of V and U_d, which better represent velocities within δ_e (e.g., $V_s = (V + U_d)/2$), however it was observed that the model outcome is robust to the precise definition of V_s. Again, for simplicity, $\delta_e = c_L V_s^2/DF$, where c_L is a proportionality constant. In summary, v_p can be estimated from the following group of equations: $v_p = (-a + \sqrt{a^2 + 4bS_p})/(2b)$, where $S_p = u_R^2/(2g\delta_e)$, $u_R^2 = \int_0^R E(\sigma)d\sigma$, and $\delta_e = c_L V_s^2/DF$. It should be noted that G09 proposes a unique value for c_L for a wide range of porous media, but it is plausible that such a constant is not universal and differs with the geometrical characteristics of the wall (e.g., c_L may be different between a canopy of vegetation and a granular wall). Using the above formulations for U_d and v_p, equation (1) can be solved iteratively to find f by varying Re, K and R/r.

3. Results

[7] With respect to GC06, the proposed model adds two more parameters pertinent to the properties of the porous wall κ_p and c_L. The former is a factor that modulates the effects of τ_p on f and therefore shifts the *f-Re* curves up or down, whereas the latter is a factor that controls the extension of the penetration depth. The larger is c_L, the smaller are S_p and v_p and ultimately, the more muted are the effects of large scale structures on f. The curves presented in Figure 3 were obtained for a granular wall with $K = 2.4 \times 10^{-8}$ m^2, $R/r = 5 - 400$, $c = 3 \times 10^{-4}$ setting $\kappa_p = 0.12$, $\phi = 0.5$ and $c_L = 0.1$. The different curves were obtained by fixing r and K but allowing R to vary. The values of r, c, K and ϕ are typical of a gravel bed described elsewhere [*Manes et al.*, 2011]. The values of κ_p and c_L were chosen arbitrarily to best reproduce the experimental curves as reported in Figure 1. Universal values could be obtained with a rigorous fitting procedure of an extensive set of experimental data, which at the moment is not available from the literature. Figure 3 also includes the results from the GC06 model for an equivalent impermeable wall with the same R/r. In the computation of f for the impermeable wall and for τ_s, the conventional values of the GC06 model parameters were used. It should be noted that the model presented here considers walls that are much thicker than δ_e. However, it can be extended to any case by imposing a limit equal to the wall thickness in the growth of δ_e.

[8] The model can reproduce the typical curves observed from experiments and it is robust to the choice of κ_p and c_L. The s-shape can now be explained as a combined effect of low values of R/r and permeability (see the thick black line in Figure 3, top). At low R/r (i.e., at $R/r < 10$, which is the range that has been earlier investigated experimentally), f increases with increasing Re until a plateau associated with the hydraulically rough regime is approached equivalent to those for an impermeable-rough wall. With further increase in Re, the earlier noted anomalous behavior is now initiated because the wall becomes effectively permeable to large

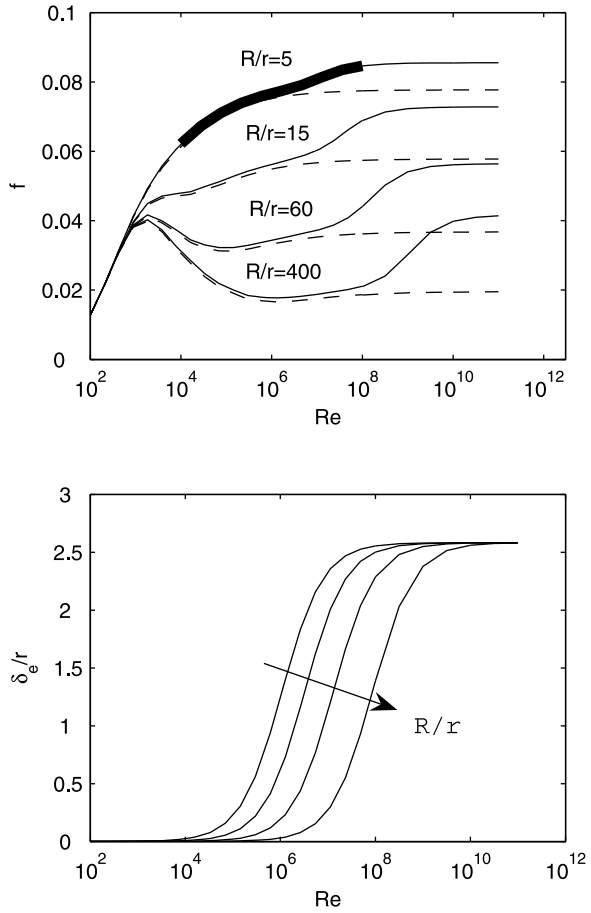

Figure 3. (top) The friction factor f versus the Reynolds number (Re) curves obtained from equation 1 (solid lines) and GC06 model (dashed lines); (bottom) the penetration depth normalized with the roughness size (grain diameter) r vs Re. The thick line highlights the part of the modelled curve that reproduces the typical shape of f vs Re curves found in the experiments.

scale sweeps and ejections, which in turn, begin to contribute significantly to momentum transport. This contribution results in further increase in f, thereby marking the rising regime. At higher values of R/r, the s-shape curve becomes less evident since in the transitional behavior f has a non-monotonic behavior, showing the so called *belly* typical of granular walls. The higher is R/r the more the friction factors f for permeable walls deviate from their impermeable counterpart. This can be explained since, for a given Re, with increasing R/r seepage velocities (i.e., U_d) generally decrease and hence momentum contrast at the interface, and ultimately friction, increases.

[9] At the limit $Re \to \infty$, the *f-Re* curves saturate reaching a Re-independent regime where the effective roughness of the wall is dictated by the size of the penetration depth δ_e, which also saturates at $Re \to \infty$ (Figure 3, bottom). Such a regime has not yet been observed experimentally, probably because it occurs at very high Re that are difficult to reach in laboratory facilities. However, we argue that, its onset should be expected. In this context, *Manes et al.* [2011] suggested that with increasing Re, turbulent structures become more energetic and may progressively penetrate the permeable wall. For such a scenario, a Re-independent f should be expected when the entire wall thickness is subjected to fluid shear. It is accepted that with increasing Re, turbulent structures increase in energy, but it is also true that the shear at the wall-interface increases and strong shear is known to promote 'wall blocking' as predicted by the "shear sheltering theory" developed by *Hunt and Durbin* [1999]. Therefore, with increasing Re, shear penetration within the wall is a result of two competing mechanisms: on the one hand, turbulence penetration is promoted because turbulence structures gain energy, on the other hand shear at the wall interface increases and this blocks turbulence structures from penetrating the permeable wall. It is conceivable that the new saturation regime in the *f-Re* curve is a region where these two effects counterbalance each other, consistent with the findings here.

[10] In the proposed model, the Re-independent regime is due to the inclusion of the quadratic term in the Forcheimer resistance law used to parameterize the drag needed in the computations of U_d, v_p and L. The inclusion of both the linear and the quadratic term is crucial to obtain the correct shape of the *f-Re* curves observed experimentally. Figure 4 demonstrates that upon neglecting the quadratic term (i.e., setting $b = 0$), f never saturates and, at high Re and low R/r, it leads to unrealistic results such as U_d being greater than V (not shown here). In contrast, neglecting the linear term (i.e., $a = 0$) leads to f being just shifted upwards with respect to their impermeable wall counterpart and hence the rising regime is lost. Therefore, the quadratic term must play the role of setting the (upper) limit that f can reach at $Re \to \infty$ whereas the linear term matches the friction factor of the equivalent impermeable rough wall to this new limit. The

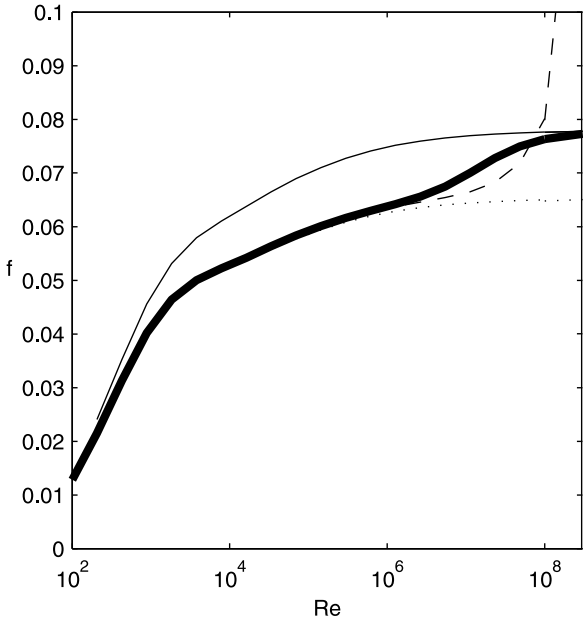

Figure 4. The influence of the linear and non linear terms in the Forcheimer resistance law on the parametrization of drag for the f versus Re curves. Dotted line is the curve for the impermeable rough case; the dashed line is for the permeable wall case without the non linear term (i.e., $b = 0$); the light solid line is for the permeable wall case without the linear term ($a = 0$) and the thick solid line is for the permeable wall with both terms. The curves were obtained for $R/r = 10$.

need for the quadratic term to reproduce realistically the experimental curves in the rising regime (i.e., at intermediate *Re*) further justifies the presence of the *Re*-independent regime at $Re \to \infty$.

4. Conclusions

[11] In turbulent flows over permeable walls, friction factor-*Re* curves are different from those reported for impermeable-rough walls. In particular, at high *Re*, they are characterized by an anomalous rising regime due to the combined effect of shear penetration and persistent viscous forces within the wall. We have presented a novel model that includes these two effects and captures well the shape of experimental *f-Re* curves provided that roughness, permeability and the Forcheimer coefficient of the wall are known. The model predicts that, at very high *Re*, the rising regime is followed by a new hydraulically rough regime where friction factors become *Re* independent. The existence of such a new flow regime still requires experimental proof. However, on the basis of physical arguments, we propose that its onset should be expected. Moreover, the model recovers the *GO*06 for impermeable walls by virtue of its construct.

[12] We conclude by pointing out that, for future practical applications, the model could be improved by: (i) providing experimentally-based parameterizations of the penetration depth δ_e, which are currently lacking - especially for granular walls and (ii) by computing τ_s with empirical formulas, such as the *Virtual Nikuradse* [*Yang and Joseph*, 2009], which match experimental data better than the GC06 model, here used as a theoretical basis to compute τ_p.

[13] **Acknowledgments.** C.M. and L.R. acknowledge the support from the Regione Piemonte (project "Giovani Ricercatori") and GK acknowledges support from the FulBright Distinguished Scholar Program and from Politechnic of Turin during his 2010 sabbatical leave, the National Science Foundation (NSF) through EAR - 1013339, AGS-110227, CBET-103347, US Department of Agriculture (2011-67003-30222), and the U.S. Department of Energy through the Office of Biological and Environmental Research (BER) program (DE-SC000697).

[14] The Editor thanks Timo Vesala and an anonymous reviewer for assisting in the evaluation of this paper.

References

Ghisalberti, M. (2009), Obstructed shear flows: Similarities across systems and scales, *J. Fluid Mech.*, *641*, 51–61.

Gioia, G., and P. Chakraborty (2006), Turbulent friction in rough pipes and the energy spectrum of the phenomenological theory, *Phys. Rev. Lett.*, *96*, 044502.

Hunt, J. C. R., and P. A. Durbin (1999), Perturbed vortical layers and shear sheltering, *Fluid Dyn. Res.*, *24*, 375–404.

Manes, C., D. Pokrajac, V. I. Nikora, L. Ridolfi, and D. Poggi (2011), Turbulent friction in flows over permeable walls, *Geophys. Res. Lett.*, *38*, L03402, doi:10.1029/2010GL045695.

Nikuradse, J. (1933), Stromungsgesetze in rauhen Rohren, *VDI-Forschungsh. 361*, VDI, Dusseldorf, Germany.

Pope, S. (2000), *Turbulent Flows*, Cambridge Univ. Press, Cambridge, U. K.

Ruff, J. F., and L. W. Gelhar (1972), Turbulent shear flow in porous boundary, *J. Eng. Mech. Div.*, *98*(EM4), 975.

Whitaker, S. (1996), The Forchheimer equation: A theoretical development, *Transp. Porous Media*, *25*, 27–61.

Yang, B. H., and D. D. Joseph (2009), Virtual Nikuradse, *J. Turbul.*, *10*, 1–28.

Zagni, A. F. E., and K. V. H. Smith (1976), Channel flow over permeable beds of graded spheres, *J. Hydraul. Div.*, *102*, 207–222.

Zippe, H. J., and W. H. Graf (1983), Turbulent boundary-layer flow over permeable and non-permeable rough surfaces, *J. Hydraul. Res.*, *21*(1), 51–65.